JOURNAL OF THE AMERICAN WATER RESOURCES ASSOCIATION

AMERICAN WATER RESOURCES ASSOCIATION

A Long View of Southern California Water Supply: Perfect Droughts Revisited

C.A. Woodhouse, D.M. Meko, and E.R. Bigio

Research Impact Statement: Concurrent or perfect droughts, lasting up to nine years have occurred in the Sacramento and Colorado River Basins, and Southern California over the past nine centuries.

ABSTRACT: The impact of drought on water resources in arid and semiarid regions can be buffered by water supplies from different source regions. Simultaneous drought in all major source regions — or perfect drought — poses the most serious challenge to water management. We examine perfect droughts relevant to Southern California (SoCal) water resources with instrumental records and tree-ring reconstructions for the Sacramento and Colorado Rivers, and SoCal. Perfect droughts have occurred five times since 1906, lasting two to three years, except for the most recent event, 2012–2015. This number and duration of perfect droughts is not unusual in the context of the past six centuries. The modern period stands out for the relatively even distribution of perfect droughts and lacks the clusters of perfect drought documented in prior centuries. In comparison, perfect droughts of the 12th Century were both longer (up to nine years) and more widespread. Perfect droughts of the 20th and 21st Centuries have occurred under different oceanic/atmospheric patterns, zonal and meridional flow, and ENSO or non-ENSO conditions. Multidecadal coherence across the three regions exists, but it has varied over the past six centuries, resulting in irregular intervals of perfect drought. Although the causes of perfect droughts are not clear, given the long-term natural variability along with projected changes in climate, it is reasonable to expect more frequent and longer perfect droughts in the future.

(KEYWORDS: streamflow; drought; climate; tree rings; Southern California.)

INTRODUCTION

The challenges of balancing water supply and demand are especially acute in the arid and semiarid regions of the western United States (U.S.) where local supplies may not be sufficient to meet demands. Evolving water needs concerning issues such as environmental flows and tribal water rights, along with prolonged drought and warming trends, have made this balance increasingly difficult to achieve. Many regions have a history of transporting surface water from distant sources to provide water, initially for agriculture, and increasingly, to support industry, energy, and urban populations. A water portfolio with a diversity of sources, including local groundwater and mountain headwaters, is often considered a buffer against droughts that could impact multiple source regions differently, depending on drought extent and drivers.

Southern California is one such semiarid region with a diversity of water supplies, relying on local groundwater and imported surface water from the Colorado River Basin and Sierra Nevada watersheds in the northern and central part of the state. The western half of Southern California (here, called SoCal) is dominated by a Mediterranean climate, with an annual average rainfall of about 480 millimeters (PRISM Climate Group, Oregon State University. Accessed 11/28/2018, http://prism.oregonstate.edu),

Paper No. JAWRA-19-0025-P of the *Journal of the American Water Resources Association* (JAWRA). Received February 12, 2019; accepted December 3, 2019.

School of Geography and Development (Woodhouse), and Laboratory of Tree-Ring Research (Meko), University of Arizona, Tucson, AZ, USA; and Department of Natural Resources and Environmental Science (Bigio), University of Nevada-Reno, Reno, NV, USA (Correspondence to Woodhouse: conniew1@email.arizona.edu).

Citation: Woodhouse, C.A., D.M., Meko, and E.R., Bigio. 2019. "A Long View of Southern California Water Supply: Perfect Droughts Revisited." *Journal of the American Water Resources Association* 1–18. https://doi.org/10.1111/1752-1688.12822.

most of it falling in the winter months. In the eastern part of the region, which includes the Imperial Valley, a desert climate prevails, with rainfall totals of <130 mm annually (PRISM Climate Group, Oregon State University. Accessed 11/28/2018, http://prism.oregonstate.edu). Imperial Valley agriculture uses about 70% of California's Colorado River allocation. The Imperial Irrigation District is the main water provider for this region, and its entire water supply comes from the Colorado River (Imperial Irrigation District, Water Supply. Accessed 3/8/2018, http://www.iid.com/water/water-supply). The Imperial Valley is a major source of produce for the U.S. in winter, bringing in over $2 billion a year (Perry, T., Despite drought, water flowing freely in Imperial Valley. Los Angeles Times, April 13, 2015, Accessed 1/5/2018, http://www.latimes.com/local/california/la-me-drought-imperial-valley-20150412-story.html). The focus of this paper is the SoCal region.

In SoCal, the main urban water wholesaler is the Metropolitan Water District (MWD), a cooperative of 26 member agencies. MWD supplies more than 50% of the region's water, serving 19 million people across six counties, including Los Angeles, Orange, San Diego, Riverside, San Bernardino, and Ventura counties (MWD, Overview. Accessed 1/5/2018, http://www.mwdh2o.com/Who%20We%20Are%20%20Fact%20Sheets/MWD_Overview.pdf). Of MWD's water supply, all comes from either the State Water Project (originating in the Sierra Nevada) or the Colorado River Aqueduct (originating in the upper Colorado River Basin). About 35% of the region's potable water comes from groundwater, developed by local water agencies (the balance is from recycled water and desalinization) (MWD, Sources of Supply. Accessed 1/5/2018, http://www.mwdh2o.com/AboutYourWater/Sources%20Of%20Supply/Pages/default.aspx). An additional source of imported surface water for the City of Los Angeles is the Owens River.

SoCal has been particularly hard hit by severe drought over the years 2012–2016, with water year precipitation averaging 59%, compared to 78% in the Sacramento River Basin, and 75% statewide (California Climate Tracker, https://wrcc.dri.edu/Climate/Tracker/CA/). This region was the last part of California to experience a break in drought in 2017 (Kim, K. and T.S. Lauder, 275 California drought maps show deep drought and recovery. Los Angeles Times, April 7, 2017. Accessed 1/5/2018. http://www.latimes.com/local/lanow/la-me-g-california-drought-map-htmlstory.html). After a brief respite in 2017, dry conditions returned to the region in 2018 (California Department of Water Resources, Water Year 2018: Hot and Dry Conditions Return. Accessed 11/28/2018, https://water.ca.gov/News/News-Releases/2018/Oct-18/Water-Year-2018). During the period of recent drought, Colorado and Sacramento River flows were below the long-term average for four years in a row (2012–2015). Flows were extremely low in the Colorado during 2012 and 2013 (<60% of average, U.S. Bureau of Reclamation, Accessed 1/5/2019, https://www.usbr.gov/lc/region/g4000/NaturalFlow/current.html) with some recovery in 2014 and 2015, whereas the reverse was true for the Sacramento, particularly in 2015, when Sierra Nevada seasonal snowpack averaged just 16% of the 31-year average (Margulis et al. 2016). SoCal water year precipitation was particularly low in 2013 and 2014, averaging <50% of average.

Although SoCal suffered extreme precipitation deficits over 2012–2016 along with high temperatures that further exacerbated moisture deficits, reducing snowpack, and soil moisture (Griffin and Anchukaitis 2014; Belmecheri et al. 2016), concurrent moisture deficits in the three main source regions were variable enough to alleviate the impacts of the recent drought in this region. The acquisition of senior water rights and development of remote water supplies has been sufficient to augment local groundwater, thus providing a buffer against the impacts of drought throughout SoCal (Gottlieb and FitzSimmons 1991). In addition, urban water utilities employed a range of management strategies during these drought years to make up for reductions in water deliveries from the State Water Project, which dropped as low as 5% in 2014, including voluntary water conservation, withdrawal of banked groundwater, and water market transfers (Lund et al. 2018). However, the resilience of this region to drought may eventually be affected by sustained west-wide drought exacerbated by warming conditions leading to declines in snowpack and greater demand for water.

A decade ago, MacDonald et al. (2008) coined the term "perfect drought" for SoCal, which they defined as prolonged and concurrent drought in the key water supply regions of the upper Colorado River and Sacramento River Basins, along with SoCal. Using paleoclimatic data, they compared conditions in these three regions, and focused on the medieval period to document decades long perfect droughts over the 11th and 12th Centuries. We have built on the work of MacDonald et al. (2008), updating and developing new reconstructions of streamflow and precipitation for these three source regions with an expanded network of tree-ring collections. The updated reconstructions now include the recent drought event, enabling us to more closely assess the occurrence of perfect drought conditions in SoCal over the past 900 years and place instrumental period droughts in a long-term context.

Specifically, we ask:

1. Have perfect droughts occurred in the instrumental period?

2. What oceanic/atmospheric conditions are associated with perfect droughts?
3. What is the nature of perfect droughts of the past six to nine centuries, and how do these compare to those of the instrumental period?
4. Have certain periods of time in the past six centuries been more prone to perfect droughts?

We start by investigating concurrent, or perfect drought conditions across the three source regions, SoCal, the Sacramento River Basin, and the upper Colorado River Basin (above Lees Ferry) over the instrumental record (1906–2017) (Figure 1). We examine the oceanic/atmospheric conditions that are associated with moisture variability in the three regions separately to gain an understanding of the region-specific conditions that coincide with drought. We then evaluate the conditions that have characterized years of perfect drought to determine what makes the circulation patterns during these events different. In the second half of the paper, we employ tree-ring reconstructions of SoCal water year precipitation, along with water year streamflow reconstructions for the Sacramento and upper Colorado River Basins to first examine the occurrence of three-region perfect droughts over the past six centuries. We evaluate the frequency of these events and clusters of perfect droughts to place the instrumental period events in a long-term context. We then use a set of longer, but less skillful reconstructions to evaluate the occurrence of perfect drought over the 12th to 14th Centuries, coinciding with the second half of the medieval period. Finally, we investigate the phasing of hydroclimatic conditions to assess whether drought (perfect or otherwise) is embedded within in-phase cyclic moisture variations in the three regions.

DATA AND METHODS

Instrumental Data, Perfect Droughts, and Circulation Analyses

In order to assess perfect droughts of the instrumental period, climatic and hydrologic data for the three regions were examined for the years 1906–2017. This study utilized three regional hydroclimatic metrics: (1) precipitation for SoCal defined by the SoCal Coast Hydrologic Unit (HU Code [HUC] level 4), (2) the Sacramento River Index (the sum of streamflow at Sacramento River at Bend Bridge, Feather River inflow to Lake Oroville, Yuba River at Smartville, and American River inflow to Folsom Lake, California), and (3) Colorado River streamflow at Lees Ferry, representing flow from the upper Colorado River Basin (Figure 1). Annual values based on the water year (October–September) were used for precipitation and streamflow. For Sacramento and Colorado River streamflow, estimates of natural flow were obtained from the California Department of Water Resources (Accessed 11/28/18, https://cdec.water.ca.gov/) and the U.S. Bureau of Reclamation (Accessed 11/28/18, https://new.azwater.gov/news/articles/2018-18-07, June 28 briefing), respectively. Precipitation rather than streamflow was used to represent SoCal drought because of the lack of a sufficiently long representative natural flow record there. Precipitation data for SoCal are from the PRISM dataset (Daly et al. 2008; 4 km resolution grid points) for the SoCal Coast Hydrologic Unit (obtained from the Westwide Drought Tracker, Abatzoglou et al. 2017).

For the instrumental period analysis of perfect droughts, water year streamflow and precipitation series were first converted to percentiles, and years with all three series below the 50th percentile were identified as years of common drought. The focus in this study was primarily on sets of two or more consecutive years of common drought, and these sets of years were defined as the instrumental-period perfect droughts.

To evaluate the atmospheric/oceanic circulation conditions associated with droughts for each region and perfect droughts across all three regions, sea surface temperature (SST) and mid-atmospheric pressure (500 mb geopotential heights) patterns were assessed using correlation fields and composite maps for key drought years. Geopotential height is roughly equivalent to the height of a pressure surface above mean sea level. Maps of heights for the 500 mb surface show positions of highs and lows of upper-air atmospheric pressure associated with changes in the jet stream, development of storms, and delivery of moisture. The HADlSST dataset was used for global SST patterns (Rayner et al. 2003). NCEP/NCAR Reanalysis data (Kalnay et al. 1996) were used for analyses of Northern Hemisphere 500 mb geopotential heights for years after 1948, whereas data from the Twentieth Century Reanalysis (V2) dataset were used for the 1930s drought composite map (Compo et al. 2011).

Correlation field maps using Northern Hemisphere 500 mb gridded data and global SSTs for the cool season (October–April, 1949–2012) were generated to identify circulation patterns associated with water year flow or precipitation variability in each of the three regions. Composite SST and 500 mb maps were generated for sets of years in which hydroclimatic values for all three basins were < the 50th percentile (i.e., perfect droughts). In these maps, SST and 500 mb values are shown as anomalies relative to the

FIGURE 1. Study region, including upper Colorado River Basin, Sacramento River Basin, and Southern California (SoCal) Coast Hydrologic Unit (the three shaded areas). San Gabriel Dam and Lees Ferry are marked with a triangle. HUC, hydrologic unit code.

1981–2010 base period. Correlation field and composite maps were generated using the NOAA/OAR/ESRL PSD Climate Analysis and Plotting Tools (Accessed 11/28/2018, https://www.esrl.noaa.gov/psd/cgi-bin/data/getpage.pl).

Paleoclimatic Data and Perfect Droughts

Tree-ring-based reconstructions of Sacramento River Index (Meko et al. 2014, Klamath/San Joaquin/Sacramento Hydroclimatic Reconstructions from Tree Rings, Final Report to California Department of Water Resources. Accessed 12/15/2019, https://cwoodhouse.faculty.arizona.edu/content/california-department-water-resources-studies) and Colorado River at Lees Ferry water year were used, along with a reconstruction of water year precipitation for a gage at San Gabriel Dam, to represent SoCal (Meko et al. 2018, SoCal Tree-Ring Study, Final Report to California Department of Water Resources. Accessed 12/15/2019, https://cwoodhouse.faculty.arizona.edu/content/california-department-water-resources-studies). In the instrumental records, the correlation between water year precipitation for the SoCal Coast HUC and at San Gabriel Dam is $r = 0.97$ (1938–2015, $p < 0.01$), so the San Gabriel Dam reconstruction is considered to be representative of the SoCal region.

Reconstructions were generated by a statistical approach described briefly here and in more detail in prior reports (as above, Meko et al. 2014; 2018). Reconstructed predictand (flow or precipitation) was linearly interpolated from a smoothed scatterplot of the observed predictand on a multisite average of standard tree-ring chronologies scaled beforehand by stepwise regression (Weisberg 1985) into separate estimates, or single-site reconstructions (SSRs) of the predictand. Each of these SSRs had in turn been generated by stepwise multiple regression of the predictand on a standard tree-ring chronology, with lagged predictor terms included to allow for autocorrelation in the tree rings or for lagged response of tree growth to climate (e.g., Meko 1997; Meko et al. 2011, 2001, 2007). The scatterplot smoothing for the final reconstruction was accomplished by locally weighted piecewise linear regression (loess; Cleveland 1979; Martinez and Martinez 2002). For the Colorado River and San Gabriel precipitation reconstructions, four different loess models were estimated. Each model was based on sets of tree-ring chronologies covering different specified spans of years. The resulting

overlapping reconstructions were spliced together, with priority assigned to the model with the highest accuracy as given by an ad-hoc variance-explained statistic: $R^2 = 1 - (\text{SSE/SST})$, where SSE is the sum-of-squares (sos) of model residuals and SST is the sos of departures of observed predictand from its calibration mean. A similar reconstruction method was used for the Sacramento reconstruction, except that more than four loess models were developed. For the Sacramento, different loess models were fit for any period covered by a unique set of tree-ring chronologies. Skill of the reconstruction models on data not used for calibration was checked with cross-validation (Michaelsen 1987; Meko 1997), and a reduction-of-error statistic measuring ability of the reconstruction model to outperform a null model consisting of substitution of the calibration mean of the predictand as the reconstructed value in each year (Fritts et al. 1990).

For each region, we developed two versions of the spliced reconstructions, each based on overlapping models. The first reconstruction was based on a large number of tree-ring chronologies with time coverage back to the early 1400s, and the second was based on a smaller set of chronologies with time coverage back to at least the early 1100s. These two versions offer a tradeoff between length and skill (Table 1). The most skillful reconstructions are used for most of the analyses in this paper, whereas the longest versions are used to investigate droughts of the medieval period. The Sacramento River and San Gabriel Dam precipitation reconstructions share a small number of predictor chronologies, which makes the relationship between the reconstructions slightly stronger than between the observed records (over 1906–2012: observed $r = 0.561$; most skillful reconstruction $r = 0.639$; long reconstruction $r = 0.603$). The reconstructions were converted to percentile values for the years 1416–2012 (using the most skillful reconstructions), and for 1126–2012 (using the longest reconstructions). As with the instrumental data, sets of consecutive years in which values for all three series were less than the 50th percentile were identified as perfect droughts for the past six centuries. The longer, less skillful reconstructions were analyzed for the 12th–14th Centuries in the same way.

Hydroclimatic Coherence among the Three Regions

Concurrence of moisture variations as a function of frequency was assessed with cross-wavelet analysis and the wavelet-transform coherency (WTC; Grinsted et al. 2004), which is analogous to correlation as a function of time and frequency. The WTC for pairs of reconstructed hydroclimate series was applied to determine if wet periods or dry periods tend to be synchronous across the three regions. Associated variations in the time domain were summarized with plots of reconstructions smoothed with a Gaussian filter of specified frequency response (Mitchell et al. 1966). Specifically, we used a 9-weight Gaussian filter with a 50% frequency response at a wavelength of 10 years. This filter emphasizes variations at decadal and longer time scales and smooths out more rapid fluctuations. Cross-wavelet analyses was done with the aid of the Matlab-based wavelet package developed by Grinsted et al. (2004) and made available for download by the National Oceanography Centre (Accessed 1/29/2019, http://noc.ac.uk/using-science/crosswavelet-wavelet-coherence).

The spatial extent of drought during several key periods was assessed using the reconstructed drought area index (DAI; Cook et al. 2010) for a six-state region (California, Nevada, Utah, Colorado, New Mexico, and Arizona). (Note that the DAI and hydroclimatic reconstructions are not completely independent.) In the DAI measure, the areal extent of drought is defined as the percentage of area with a Palmer Drought Severity Index (PDSI; Palmer 1965) of −1.0 or less (Cook et al. 1997).

RESULTS AND DISCUSSION

Instrumental Period Perfect Drought

Throughout the 20th and early 21st Centuries, major periods of drought have affected SoCal, the Sierra Nevada headwaters of the Sacramento River, and the upper Colorado River Basin. Perfect drought conditions occurred within each of five major

TABLE 1. Reconstruction span of years with calibration/verification statistics.

	Most skillful				Longest			
Reconstruction	**Start**	**End**	R^2	**RE**	**Start**	**End**	R^2	**RE**
Colorado River at Lees Ferry	1416	2015	0.81	0.80	1116	2014	0.58	0.55
San Gabriel Dam precipitation	1405	2016	0.80	0.78	1126	2015	0.60	0.57
Sacramento River Index	1405	2010	0.75	0.72	900	2012	0.71	0.68

Note: RE, reduction-of-error.

droughts over the 1906–2017 instrumental period (Figure 2). Drought events play out differently from region to region, and typically, the most severe drought in one region (in terms of persistence and deficits) is less severe in the other regions. For example, drought conditions in the late 1920s and 1930s were severe and prolonged in northern California, with consecutive below median flows in 1929–1934 (Figures 2 and 3a). The upper Colorado River Basin experienced very low flows in 1931 and 1933–1935, but the drought was broken by 1932, which was quite wet. In SoCal, only the years 1933 and 1934 were dry. Thus, these two years were the perfect-drought years for this period (Figure 3a). The most extreme five-year drought in SoCal occurred from 2012 to 2016 (Figure 3e). Colorado River flows were below the median over this period, but deficits were quite moderate in several years, whereas Sacramento River flows were quite low from 2012 to 2015, but above the median in 2016. Conditions were below the median in all three basins over the four-year period, 2012–2015, and this is the longest perfect drought in the instrumental record. Besides the 1930s and 2010s, there are three other perfect droughts with flow or precipitation below the median in all three basins: 1959–1961, 1976–1977, and 1989–1990 (Figure 3b, 3c, and 3d). Each perfect drought varies in length and character, and is bracketed by variable drought conditions in the individual basins.

Circulation Patterns Associated with Perfect Drought

When circulation patterns associated with water year flow or precipitation in each of the three basins are examined, general similarities are evident in 500 mb pressure, with some subtle differences (Figure 4, top). The 500 mb pressure correlation patterns over the North Pacific and North America during the cool season are relatively similar for all three regions. The dominant feature is a correlation between streamflow or precipitation and a pressure center on or slightly off the coast of western North America. These results indicate that during dry years, high pressure likely directs the jet stream to the north of all three regions. A pressure center with the opposite sign of correlation centered over the Hudson Bay suggests air flow is then directed south, in a meridional flow pattern across northern North America. Slight differences in the location of the pressure center anomaly reflect the basin-specific circulation most closely associated with moisture variability.

The SST correlation patterns are broadly similar as well, with positive correlations between streamflow or precipitation and SSTs in the eastern Equatorial Pacific, and negative correlations with western North Pacific and western North Atlantic SSTs (Figure 4, bottom). As with the pressure correlation patterns, there are some key differences. The SoCal correlation field is strongly indicative of an ENSO teleconnection pattern, a pattern that is more muted for the Sacramento River. In addition, SSTs south of the Gulf of Alaska appear to be negatively associated with Sacramento flow, whereas SSTs south of the Alaskan Peninsula show a positive association. In contrast, the SST pattern associated with Colorado River flow is less indicative of ENSO, with positive correlations just south of the equator in the eastern Pacific and south of the Alaskan Peninsula, as for the Sacramento. The pattern of SST correlations in the North Pacific for the Colorado and Sacramento Rivers may be an indication of the greater importance of extratropical Northern Hemisphere circulation for these two basins, compared to the SoCal region, for which ENSO phase may be more important.

Composite maps for the perfect-drought years show that several different circulation patterns characterize these widespread events (Figure 5). In all cases, a high pressure anomaly is located just off the coast of the Pacific Northwest, sometimes as a discrete center and in other cases, as a band of high pressure across the North Pacific. During the 1959–1961 and 1976–1977 droughts (Figure 5b and 5c), this high pressure is weaker, but along with a strengthened Aleutian low, is part of a wave train of high and low pressure centers across the upper mid-latitudes. This suggests a meridional flow pattern with a blocking ridge over the West Coast. During the 1989–1990 and 2012–2015 droughts (Figure 5d–5e), northern hemisphere circulation is dominated by a band of high pressure from western Siberia to the West Coast of North America, and with less intensity across the North Atlantic. The average circulation pattern appears to be characterized by zonal flow, with the jet stream to the north of all three regions.

Besides the North Pacific high pressure center, associated pressure anomalies occur elsewhere in the Northern Hemisphere, but are variable among perfect droughts. For example, perfect droughts occurring after 1950 are associated with contrasting anomalies reflecting the Northern Atlantic Oscillation (NAO; Barnston and Livezey 1987; monthly NAO indices, 1950–2018, Climate Prediction Center. Accessed 12/17/2018, http://www.cpc.ncep.noaa.gov/data/teledoc/telecontents.shtml) in different ways. The NAO is an oscillation in sea level pressure between polar high pressure over Iceland and tropical low pressure over the Azores (Hurrell 1995; Visbeck et al. 2001). It is a part of the hemispheric mode of variability known as the Arctic Oscillation, which influences winter circulation in the Northern Hemisphere (Thompson and Wallace 1998; Quadrelli and Wallace 2004). The

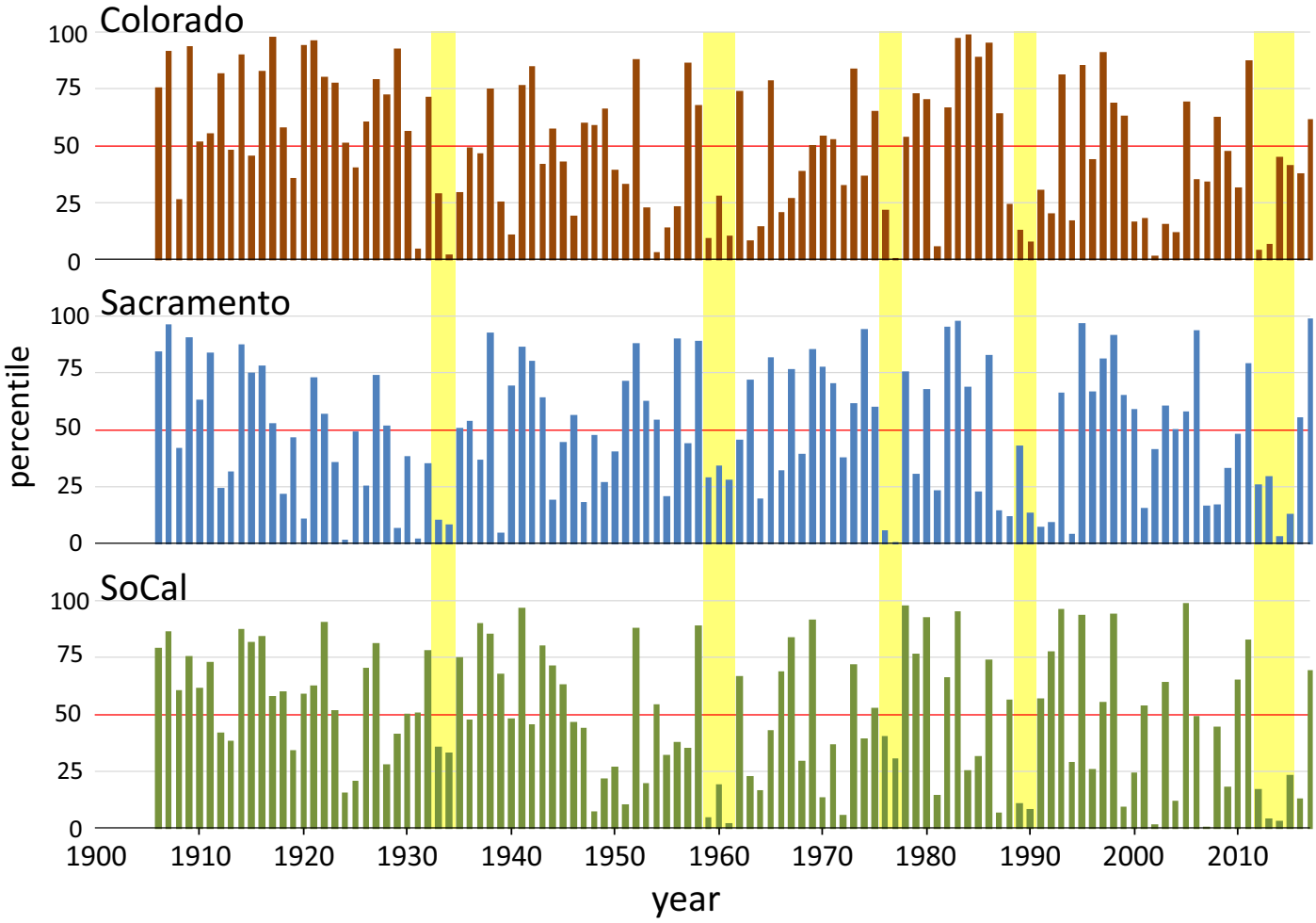

FIGURE 2. Water year streamflow and total precipitation, 1906–2017, in percentile for Colorado River at Lees Ferry (top), Sacramento River Index (middle), and SoCal Coast HUC (bottom). Perfect droughts (<50th percentile in all three regions for two or more consecutive years) are indicated by vertical shading.

1959–1961 and 1976–1977 droughts were characterized by negative phase NAO (a weak pressure gradient, more meridional flow), with each drought containing a year in the lowest decile of 1950–2018 winter (December–February) NAO. In contrast, the 1989–1990 and 2012–2015 droughts were characterized by positive phase NAO, with each drought containing a year in the highest decile of NAO. This coincides with an observed positive trend in NAO over the 20th Century (Hurrell 1995; Visbeck et al. 2001).

The SST patterns associated with perfect droughts are also variable. The 1959–1961 and 1976–1977 droughts are not indicative of any particular pattern, although conditions are mostly cool in the Pacific during the 1976–1977 drought. The 1989–1990 drought (Figure 5d) is characterized by cool SSTs in the central and eastern Equatorial Pacific, along with a pressure pattern that suggests ENSO as a driver. This drought overlapped with a strong La Niña event in the second half of 1988 and into 1989 (Wolter and Timlin 2011). The influence of La Niña conditions is also suggested in the SST (and 500 mb) patterns for the 1933–1934 drought (Figure 5a), and indeed, moderate La Niña conditions occurred over these years (Wolter and Timlin 2011). The composite SST map for most recent perfect drought, 2012–2015 (Figure 5e) shows no distinctive pattern of SSTs.

These results suggest that perfect droughts can occur under several different patterns of ocean/atmospheric circulation. Either meridional flow, with persistence of high pressure off the Pacific Northwest coast, or more zonal flow, with the jet stream likely forced to northern latitudes, are conditions that can lead to west-wide cool season drought. The SST patterns also indicate several ocean circulation patterns may interact with the atmosphere to promote persistent and widespread drought. In most droughts, cooler SSTs in the Equatorial Pacific suggests an underlying Tropical Pacific influence, with ENSO playing a role in some but not all droughts.

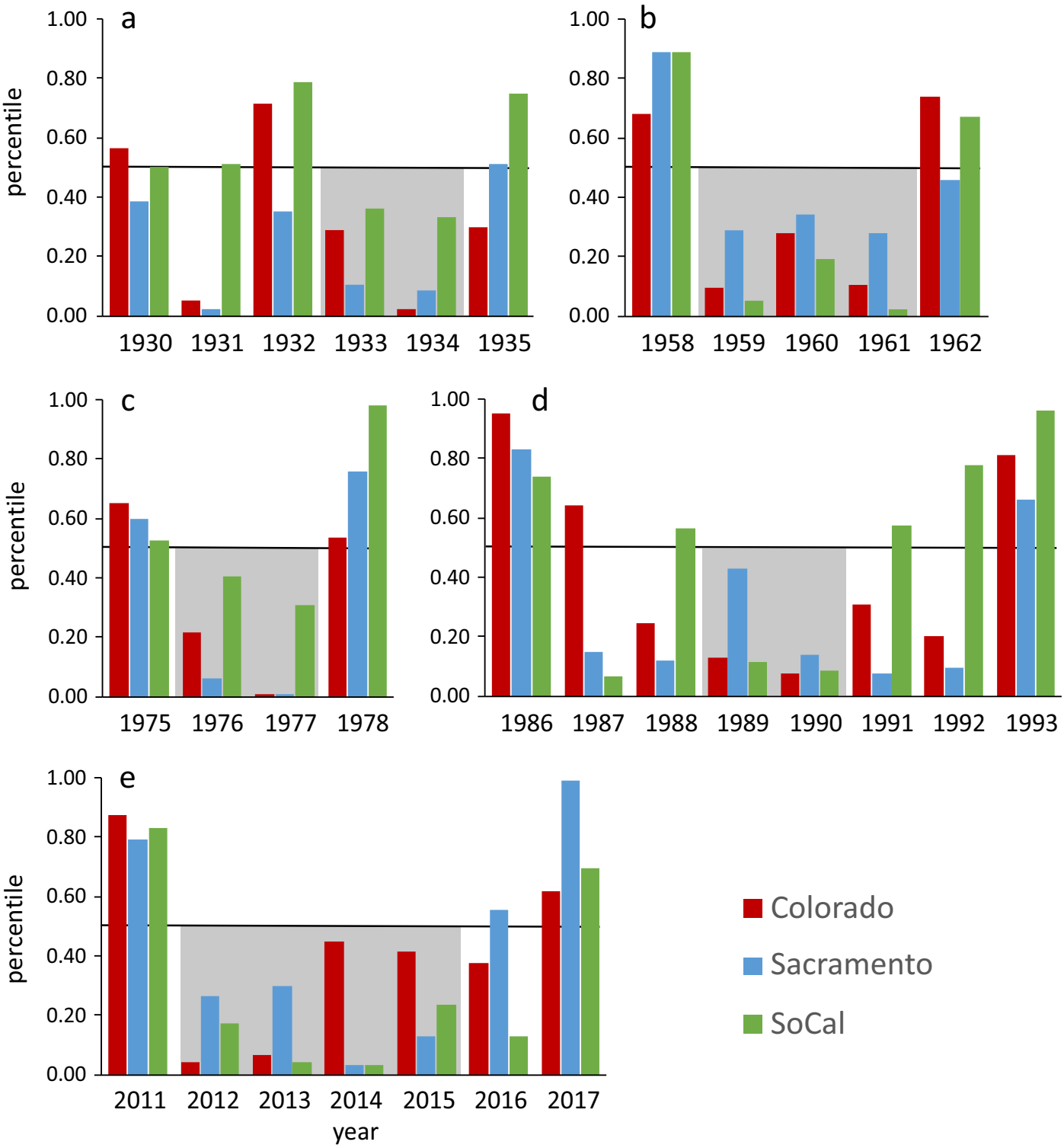

FIGURE 3. Perfect droughts of the 20th and 21st Centuries in the instrumental records. Colorado River flow (red bars), Sacramento River index (blue bars), and SoCal Coast HUC (green bars) for the five perfect droughts (gray shading), (a) 1933–1934, (b) 1959–1961, (c) 1976–1977, (d) 1989–1990, and (e) 2012–2015. Flanking years are shown for context. Values are in percentile. The black horizontal line shows the 50th percentile.

Droughts over the Past Six Centuries

Since the instrumental records for the Colorado, Sacramento, and SoCal regions are only slightly more than 100 years long and contain only five perfect drought events, it is not possible to robustly assess the frequency, duration, and distribution of perfect droughts. However extended records from tree rings

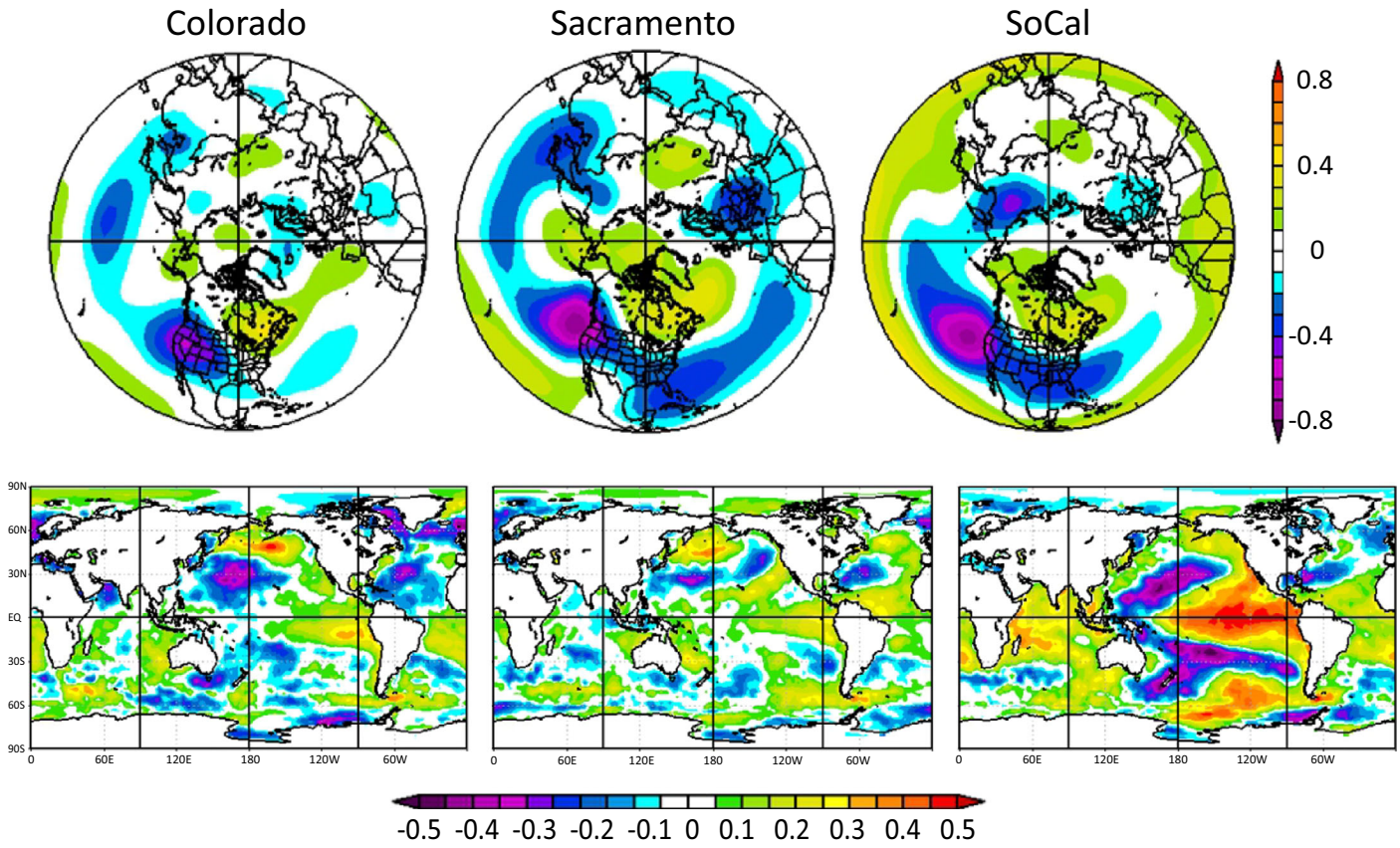

FIGURE 4. Correlation field maps showing relationship of water-year-total instrumental river flow or precipitation with October–April 500 mb geopotential height (top row) and sea surface temperature (SST) (bottom row). From left to right, time series used for correlations are (1) Colorado River natural flow at Lees Ferry, (2) Sacramento River natural flows (four-river index), and (3) precipitation for the SoCal HUC. Analysis period 1949–2012. Maps from National Oceanic and Atmospheric Administration (NOAA)/Earth System Research Laboratory (ESRL) Physical Sciences Division.

make these assessments possible, going back six centuries and, with less certainty, nine centuries.

Using the criteria of all three regions with values less than the 50th percentile for two or more years, it is evident that perfect droughts are relatively common, although not evenly distributed through time (Figure 6). There are notable gaps as well as multidecadal periods of more frequent perfect droughts. The multidecadal periods (30 years in this case) with the highest number of perfect drought events are 1630–1659 and 1708–1737, with five events each (the average frequency is just over 1.5 events per 30-year interval for the full six centuries). These two periods are separated by the longest period without a perfect drought event, 1660–1705. Neither of the two periods with the higher frequency of perfect droughts is characterized by particularly widespread drought conditions across the western U.S. The areal extent of drought (DAI) over that broad domain is 27% for 1630–1659 and 32% for 1708–1737 compared to a mean of 29% for all 30-year periods (1414–2005), suggesting these were not multidecadal periods of widespread and persistent drought. Instead, these were periods in which drought conditions coincided more often among these three regions.

The longest perfect drought lasted four years (1629–1632), indicating that while the recent perfect drought, 2012–2015, is rare, it is not unprecedented. Although it is not possible to make a direct comparison between the reconstructed and instrumental period data, average deficits over the three regions in the four-year perfect droughts were relatively similar for their respective periods, averaging in the 20th percentile for 1629–1632 and the 18th percentile for 2012–2015.

In the case of shorter events, 10 three-year drought events occurred but the distribution is markedly uneven, with seven occurring in the 18th and early 19th Centuries (1705–1824) (Figure 6). As would be expected, two-year perfect drought sequences are most common (21 events), also relatively unevenly distributed, with the highest number occurring from 1575 to 1675.

As mentioned, the distribution of perfect droughts is uneven, with several notable episodes of clustering. To study this phenomenon, we define a perfect-

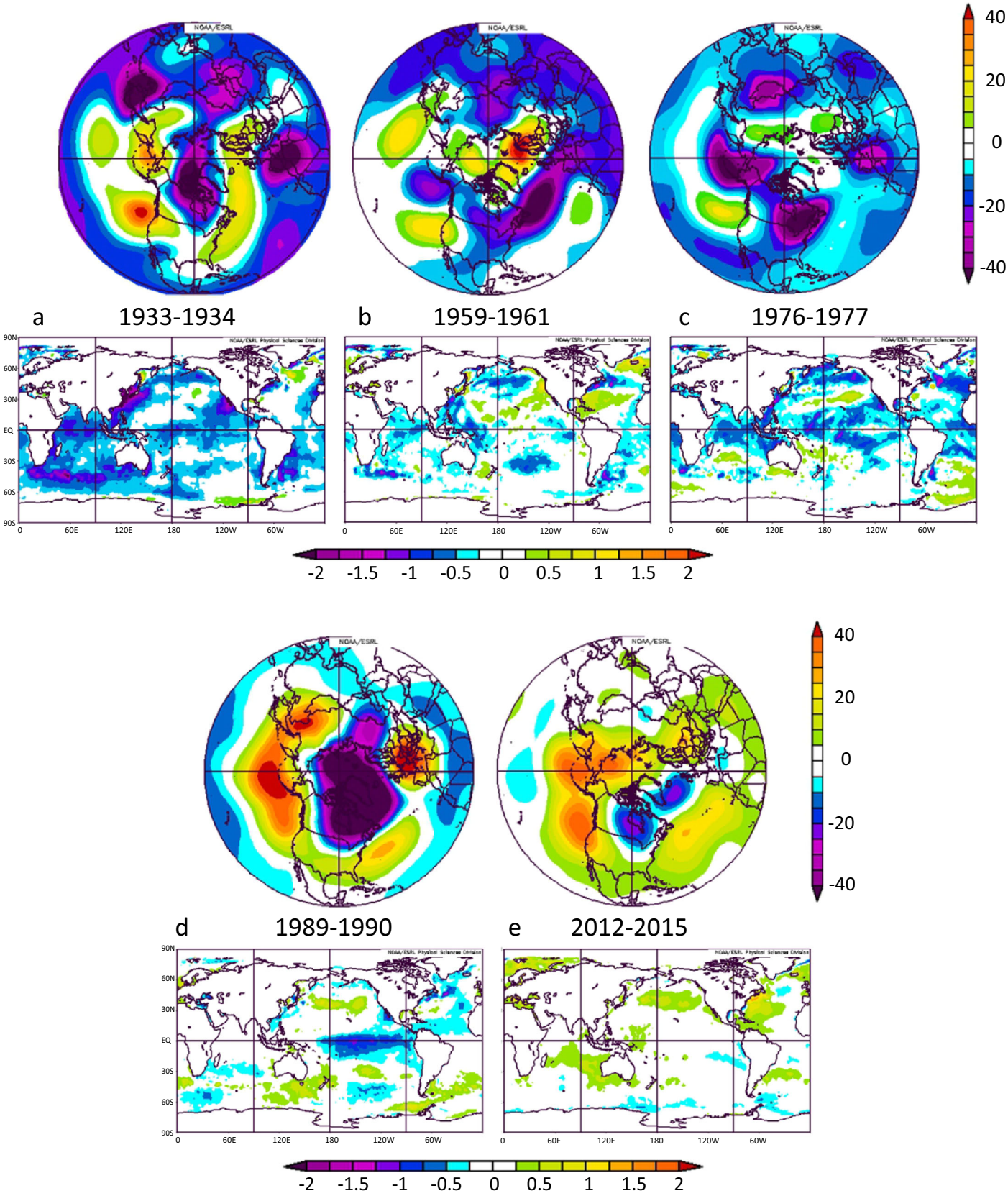

FIGURE 5. Composite maps for sets of perfect-drought years, October–April 500 mb geopotential height (m), and SST (C) anomalies (1981–2010 climatology). Perfect droughts are (a) 1933–1934, (b) 1959–1961, (c) 1976–1977, (d) 1989–1990, and (e) 2012–2015.

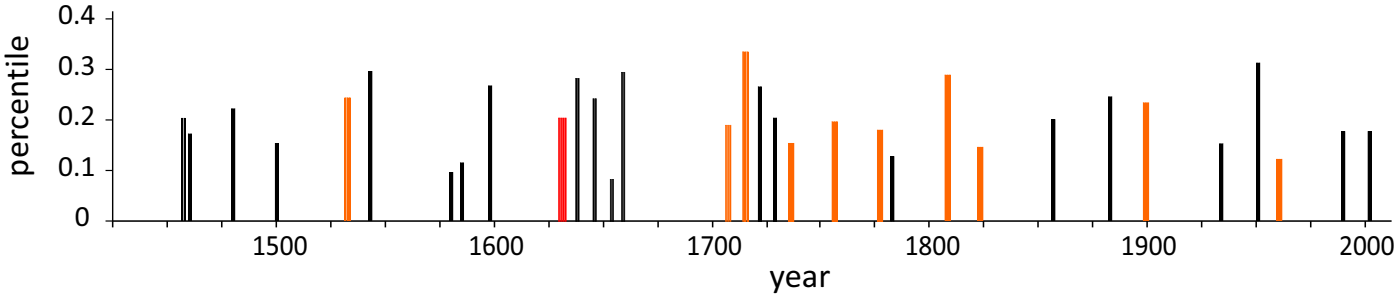

FIGURE 6. Distribution of perfect droughts, two or more years in length, 1416–2012. Vertical bars indicate the average percentile value for streamflow or precipitation in the three regions, over the years of the perfect drought. Black bars indicate two-year events, orange indicates three-year events, and red indicates a four-year event.

drought cluster as a set of single and multiyear perfect droughts separated by a year in which drought persists in only one or two of the three regions. The period 1452–1460 includes two single-year perfect droughts and two two-year perfect droughts, each broken by one year with conditions slightly above or near the median in SoCal and the Sacramento River Basin (Figure 7a). The average annual values were at the 27th percentile among all three regions, whereas the Colorado River had persistently low flows, with average annual flows at the 18th percentile for the decade ending in 1461. In 1462, conditions in all three regions rose above the median. The seven-year period, 1579–1585 (Figure 7b), is a cluster characterized by 2 two-year perfect droughts separated by a single perfect-drought year (1582) and two years with drought in at least one basin. Across all years and regions, average values fall within the 27th percentile. This was another period of especially prolonged drought in the Colorado River Basin (all seven years), and coincides with the 16th Century megadrought (e.g., Stahle et al. 2000) during which drought conditions extended across most of western North America as well as the southern Great Plains. The year 1580 was exceptionally dry for all three regions, and is also the year for which the average PDSI value reconstructed for western North America was the second lowest in the past 1000 years, after 1934 (Cook et al. 2014). The drought over this period was less severe and sustained for SoCal, which experienced two years of precipitation above the 80th percentile. A third cluster of perfect droughts occurred from 1776 to 1783 (Figure 7c), with eight years in a sequence similar to the late 16th Century; two-year and three-year perfect droughts separated by a single perfect-drought year and two years with drought in at least one region.

These analyses suggest that the frequency and duration of perfect droughts in the instrumental period is generally representative of the past six centuries, although the distribution of events is quite variable. However, the 20th and 21st Century record of perfect droughts is notable for a lack of clustering of perfect droughts, and is characterized by events that are fairly evenly spaced (Figure 6).

Medieval Period Perfect Droughts

The record of the past six centuries presents a longer context for evaluating modern period droughts, but extending these hydroclimatic records back into the medieval period (roughly 900–1400 CE) allows an assessment of perfect droughts during an interval of time known for extremely persistent and widespread droughts (e.g., Stine 1994; Cook et al. 2004; Cook et al. 2010; Woodhouse et al. 2010). When the 12th–14th Centuries are examined in the longer, but less skillful reconstructions, a different pattern is evident (Figure 8, top). Compared to the last six centuries, these three centuries display several prolonged perfect droughts, along with a long interval with no perfect droughts. The 12th Century is characterized by two severe and persistent perfect droughts, seven and nine years in length (Figure 9a and 9b), separated by only 13 years, during which there is only one year of above median values in all three basins. Averaged values for the 1130–1136 perfect drought are at the 26th percentile, while the average for the 1150–1158 drought is at the 22nd percentile. Over the interval encompassing both (1130–1158), average annual values are at only the 30th percentile. This period has been recognized as an extraordinarily persistent period of drought in the both the Colorado (Meko et al. 2007) and the Sacramento Rivers (Meko et al. 2001). It is now apparent that it affected SoCal as well. The 13th Century perfect droughts are limited to two- and three-year events, with two-year events occurring every 14 years, on average (Figure 8, top). This century includes a sequence of three perfect droughts broken by two nonperfect-drought years (Figure 9c),

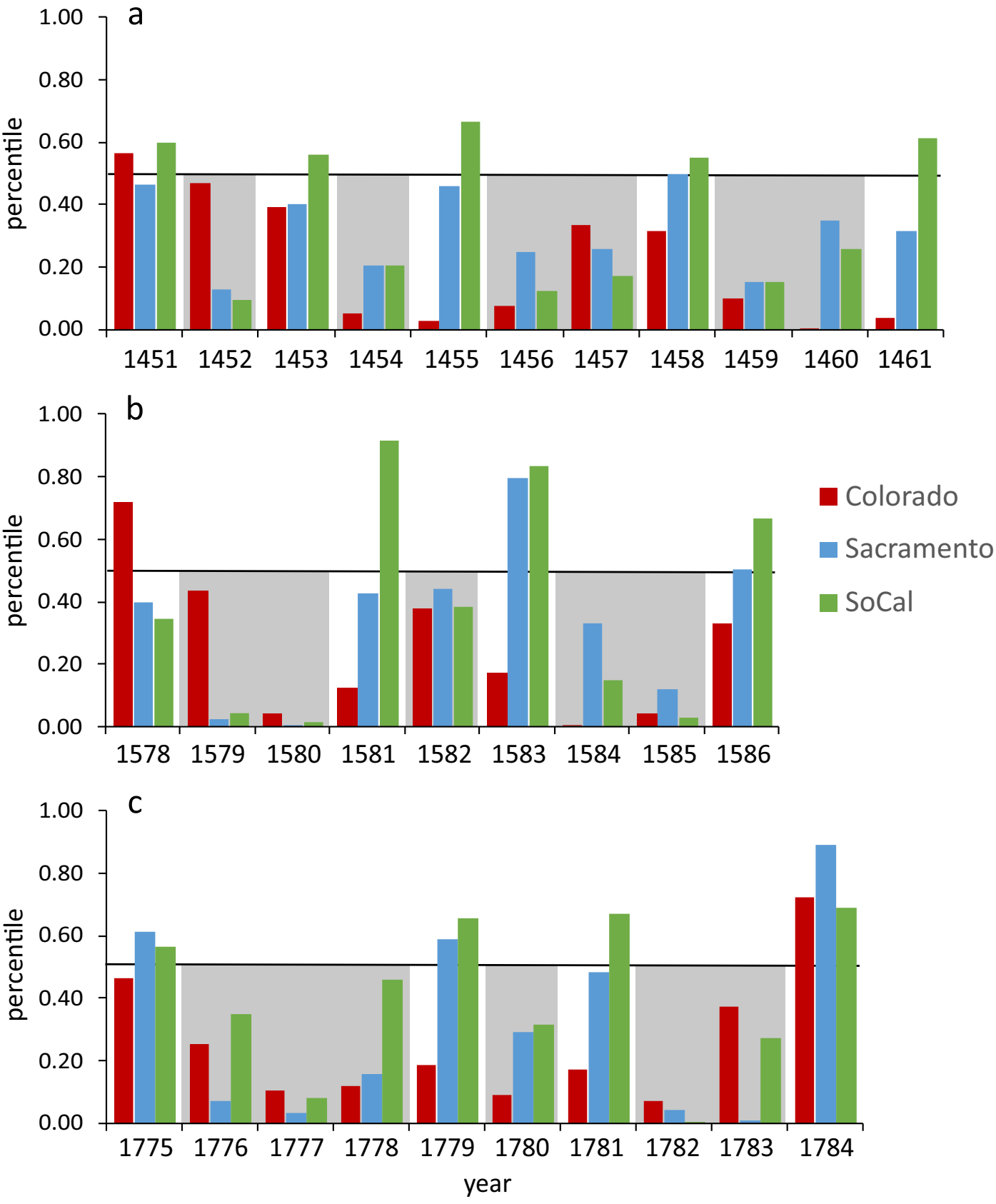

FIGURE 7. Perfect drought clusters. Colorado River flow (red bars), Sacramento River index (blue bars), and SoCal (green bars) for the three periods, (a) 1451–1461, (b) 1578–1586, and (c) 1775–1784. Perfect-drought years are in gray shading. Values are in percentile; the black horizontal line shows the 50th percentile.

somewhat similar to the perfect drought cluster in the 18th Century (Figure 7c). In contrast, the 14th Century is almost completely devoid of perfect droughts, with just 2 two-year events.

The DAI averaged over the six-state area suggests drought conditions were widespread over the years 1130–1158, with 54% of the area under drought, in contrast to the 14th Century, with a DAI averaging 26% (although spatial coherence may be somewhat enhanced due to the reduced network of tree-ring chronologies in the medieval period, Cook et al. 2007; Figure 4). The portion of the medieval period examined here (1126–1399) represents a transition from the severe, persistent, and widespread 12th Century droughts to less severe conditions similar to those of the 17th and 18th Centuries, and finally into a period that is relatively free of perfect droughts, and possibly wetter, west-wide, through the end of the 1300s. The widespread, persistent drought conditions of the 12th Century are in marked contrast to the periods of shorter, but higher frequency perfect droughts in the mid-17th and early 18th Centuries, which were not widespread across the western U.S.

Regional Hydroclimatic Coherence over Past Centuries

The temporal distributions of perfect droughts suggest periods of synchrony in drought across the Colorado, Sacramento, and SoCal regions over the past six centuries. WTC plots for the three pairs of reconstructions show that coherence between SoCal and Sacramento occurs at higher frequencies (four–eight years) and is more temporally consistent, than for the other two pairs of series (Figure 10). This in-phase coherency might be expected, given the proximity of these two California regions and a sharing of some tree-ring series in the reconstruction models. A persistent high-amplitude ridge or trough would favor similar-sign moisture anomalies along a broad latitudinal swath of California. The high-frequency coherence at four to eight years suggests ENSO as a possible driver. Correlation field maps indicate, however, that ENSO circulation is closely associated with SoCal precipitation, but not with Sacramento River flow, at least during the instrumental period. This is likely a reflection of SoCal's location in the southern part of an ENSO-related dipole, while the Sacramento River Basin is nearer to the pivot point (Dettinger et al. 1998; Wise 2010). Coherence is also evident between these two regions at multidecadal time scales. Mostly in-phase relationships are evident in the time series below the WTC plot, except for a few intervals such as the mid-15th, early 17th, and early 19th Centuries.

Coherence is much spottier between the Colorado and Sacramento, and Colorado and SoCal series. These pairs of reconstructions are free of possible artificial coherence, as their predictor tree-ring networks share no tree-ring chronologies. The Colorado and Sacramento have several intervals of coherence at decadal to multidecadal time scales, around 1500, the second half of the 1700s, the mid-1800s, and the

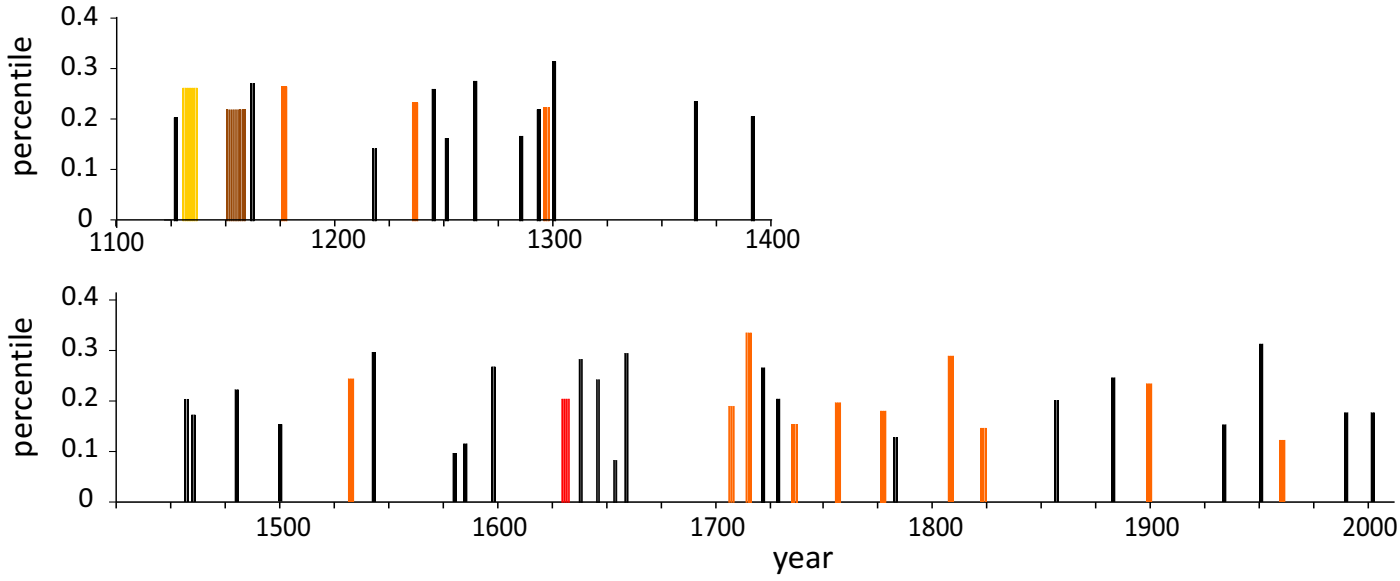

FIGURE 8. Distribution of perfect droughts, two or more years in length, top, 1126–1399, bottom 1416–2012 (same as Figure 6, for comparison). Vertical bars indicate the average percentile value for streamflow or precipitation in the three regions, over the years of the perfect drought. Black bars indicate two-year events, orange bars = three-year events, red = a four-year event, yellow = a seven-year event, and brown = a nine-year event.

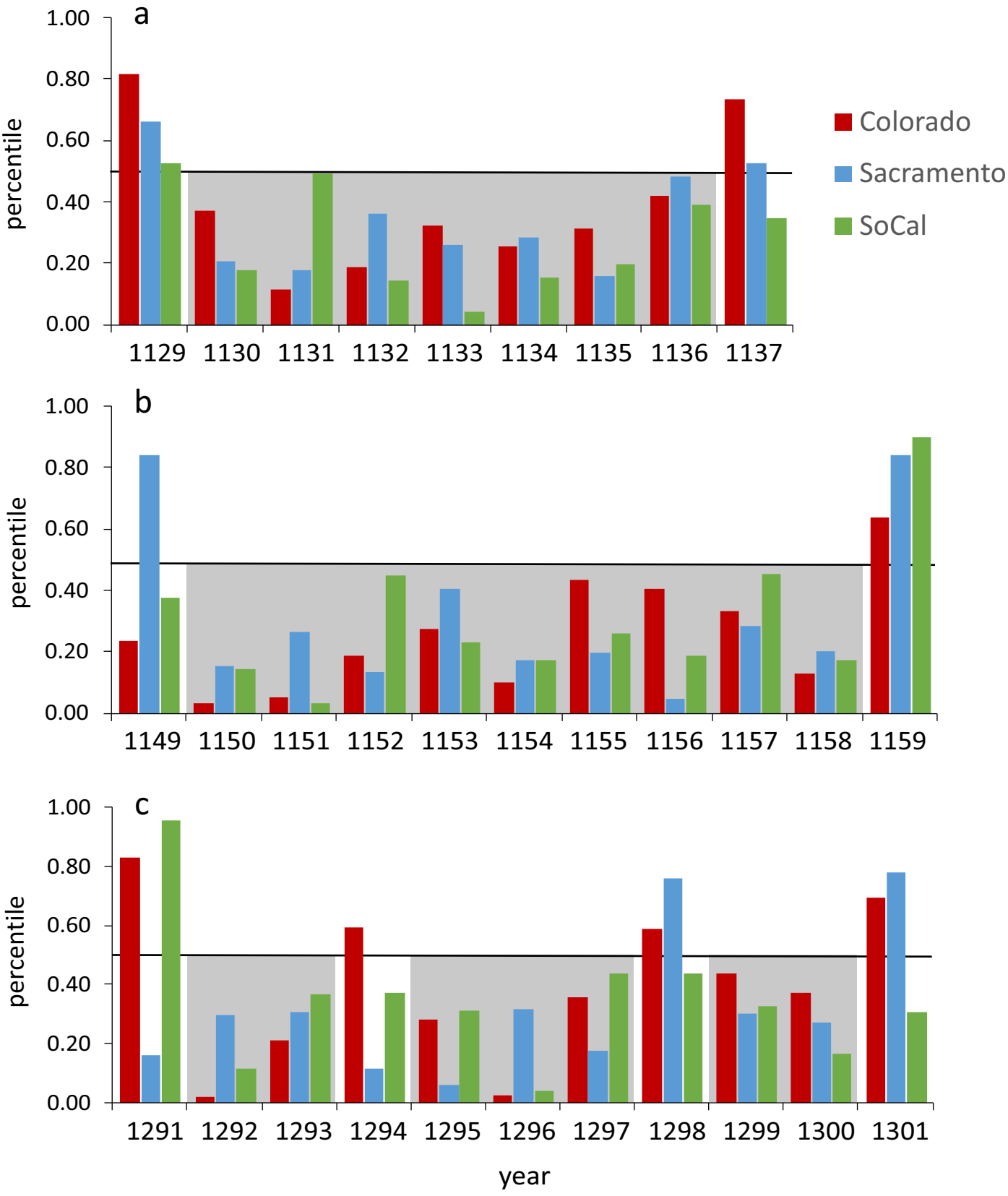

FIGURE 9. Medieval perfect droughts and clusters with flanking years (1126–1399). Colorado River flow (red bars), Sacramento River index (blue bars), and SoCal (green bars) for three periods, (a) 1129–1137, (b) 1149–1159, and (c) 1291–1301. The first two are unbroken perfect droughts, whereas 1292–1300 is a cluster broken by two intervening years with one or more regions above median. Perfect-drought years are in gray shading. Values are in percentile; the black horizontal line shows the 50th percentile.

end of the 20th Century, although in some cases, the Colorado appears to be lagging the Sacramento (Figure 10b). Similar but even less consistent relationships are seen for the Colorado and SoCal (Figure 10c). However, all three pairs share coherence at 50–70 years, particularly from the mid-1500s to about 1700, with the Colorado and Sacramento mostly in phase during this interval, and the other two pairs slightly out of phase. This period of time includes the late 1500s perfect drought cluster (Figure 7b). It is also characterized by a strong switch from the drought conditions of the late 1500s to very wet conditions in the early 1600s (Biondi et al. 2000), with a return to region-wide drought in the mid-1600s (Figure 10, time series plots below WTCs). These swings are less evident in the SoCal reconstruction where magnitudes are muted, but coherence is still present (Figure 10c). These results suggest that multidecadal coherency exists for Colorado and Sacramento River flows and SoCal precipitation at different intervals of time. Whether these are paced by a circulation mechanism or randomly synchronized is unknown, but the result has been irregular intervals of perfect droughts across the three regions.

SUMMARY AND CONCLUSIONS

Major multiyear droughts impact large parts of the western U.S., but typically, the most severe drought conditions are limited to a smaller area and/or the timing of the worst drought years is different within subregions. During each of the five major 20th and 21st Century droughts (1930s, 1950s, 1970s, 1980s–1990s, and 2010s), SoCal and the Colorado and Sacramento River Basins experienced perfect drought conditions that lasted for two or three years except for the most recent perfect drought, 2012–2015, which lasted four years.

No specific oceanic/atmospheric circulation patterns are associated with perfect droughts, and these events occur under a variety of conditions. In all cases, a dominant feature is a center of high pressure just off the Pacific Northwest coast, diverting the storm track to the north of the three study regions. Aside from this common feature, the atmospheric flow patterns can be zonal or meridional. SST patterns suggest a variable role for the equatorial Pacific, most important for SoCal, and for the 1930s and 1980s–1990s droughts, which overlapped with La Niña events. During other perfect droughts, patterns are less distinct, but cool Pacific SSTs are usually present, with a notable exception being the most recent drought.

Perfect droughts of the past 100 years do not appear to be unusual in the context of the past six centuries, with respect to duration and frequency. Both instrumental and paleoclimatic records document perfect droughts ranging from two to four years in duration. The instrumental period does not stand out in terms of the frequency of perfect drought events (numbers of events per century), but since about 1800, perfect droughts and drought clusters have been less frequent. The distribution of events within the instrumental period is relatively even, in contrast to the 17th Century when all five of the perfect droughts occurred within just over three decades. Along with evenly spaced events, the instrumental period is also characterized by a lack of perfect droughts clusters. These results suggest that the instrumental period may not accurately reflect the potential for back-to-back perfect droughts or clusters of perfect droughts to occur in the future.

The distribution and character of medieval period perfect droughts are different that those of the past 600 years, particularly in the 12th Century, which included perfect droughts lasting up to nine years. The spatial extent of the medieval perfect droughts is also notable, with over half of the western U.S. experiencing drought conditions during the 12th Century events. The medieval period has been characterized by widespread drought, increased aridity, and dustiness in the western and southwestern U.S. (e.g., Stine 1994; Cook et al. 2004, 2010; Routson et al. 2016). Northern Hemisphere and North American summer temperatures during some intervals of this period were probably warmer than any since, until the late 20th Century (Mann et al. 2008; Trouet et al. 2013; Wilson et al. 2016). Consequently, it is not surprising that 12th Century perfect drought events are much more persistent than those of the past six centuries. However, these unusually persistent perfect droughts do not occur after the 12th Century, marking the end of this regime, at least in the three regions.

With respect to coherency of moisture conditions across the three regions over the past six centuries, WTC analysis suggests that perfect drought conditions occur periodically and with varying frequencies. One notable period of coherence is between the mid-1500s to 1700s, which coincides with a phase when perfect droughts are most frequent. As mentioned above, the period of instrumental record has experienced relatively evenly spaced droughts, but it would be reasonable to anticipate the possibility of more frequent perfect droughts in the future, even considering just the past six centuries.

The results presented here are in agreement with those of MacDonald et al. (2008) with respect to observed perfect droughts and associated oceanic/atmospheric circulation conditions. Our findings also support their exploratory analysis indicating prolonged perfect droughts occurred in the medieval

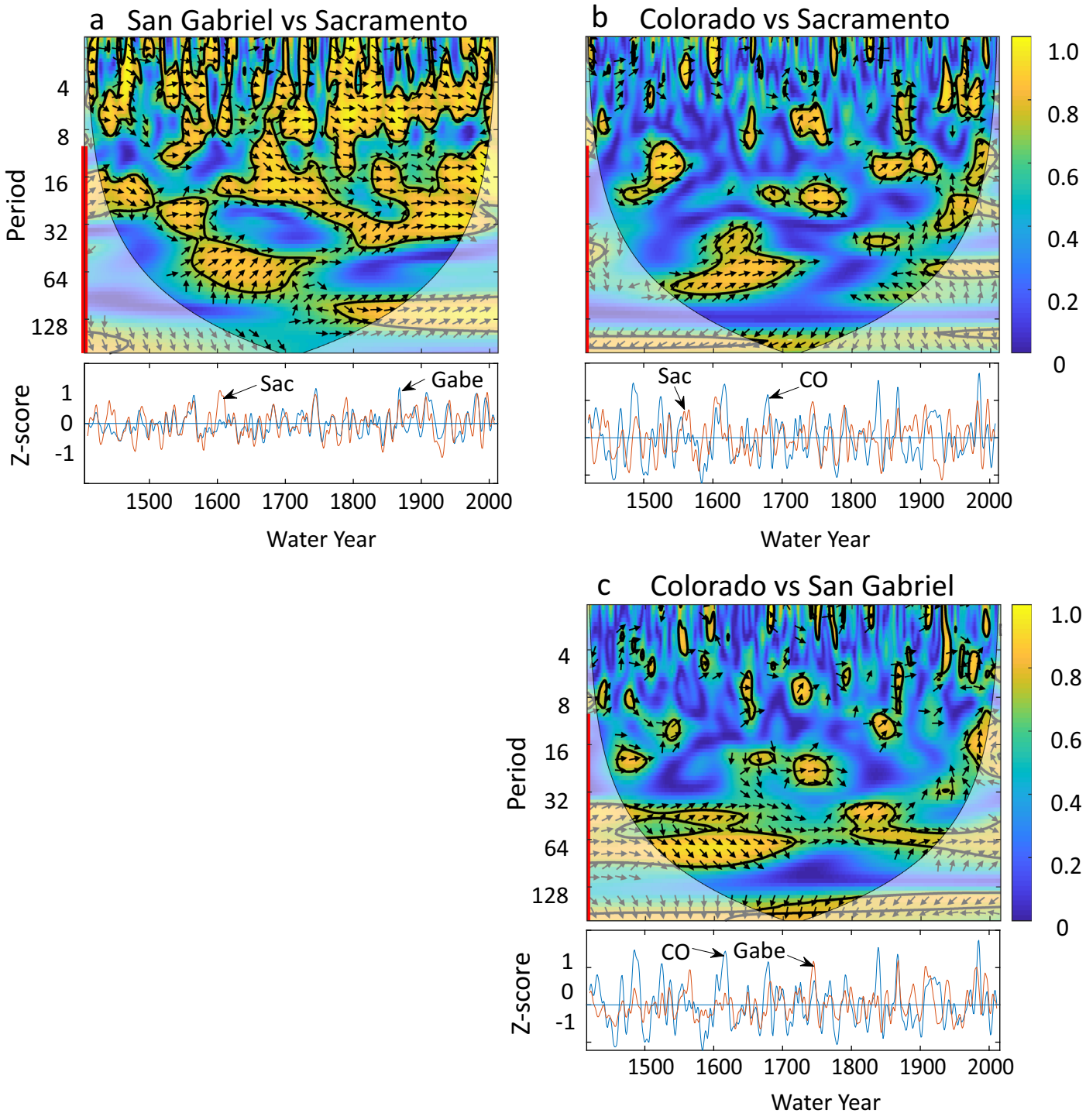

FIGURE 10. Wavelet-transform coherency (WTC) plots. (a) San Gabriel Dam precipitation and Sacramento River index (1405–2012); (b) Colorado River and Sacramento River index (1416–2012); (c) San Gabriel Dam precipitation and Colorado River (1416–2015). Scale shows coherency, with significantly high coherency marked by yellow regions bordered by a solid black line. Phase difference is marked by the direction of the arrows: arrow down to the right when first series, as listed at top of plot, leads second series. The red bar along *y*-axis indicates wavelengths emphasized by the smoothed (Gaussian) *z*-score time series plots below the WTC (i.e., decadal and longer).

period. However, our results suggest that while medieval droughts were much longer than in the instrumental record (seven–nine years vs. two–four years), these droughts were much shorter than the 30–60 year droughts reported by MacDonald et al. (2008). This may be at least partly due to the smoothing applied in their drought assessment, and also possibly to the statistical characteristics of tree-

ring data used for their exploratory reconstructions, which relied heavily upon tree species that contain a large degree of year-to-year persistence in growth (*Pinus longeava*, *P. flexilus*, *P. artistata*) (Kipmueller and Salzer 2010).

The reconstructions of Colorado and Sacramento River flow and SoCal precipitation indicate that the SoCal water supply is buffered from the impacts of perfect droughts to some extent. However, the extended records from these three water supply source regions suggest natural variability has resulted in numerous perfect droughts over the past six centuries, with some clustered into relatively short intervals of time. Perfect droughts were even more persistent during the medieval period. These types of droughts have occurred in the past, and could occur in the future. However, current temperatures are now warmer than in the past, and will continue to warm, exacerbating the impacts of moisture deficits, and increasing water demand (Cook et al. 2015; Williams et al. 2015). Projections for Colorado River flow point to decreasing runoff, even if precipitation remains the same, with an increasing risk of decadal and multidecadal drought (Udall and Overpeck 2017). Likewise, water supplies in the central and northern parts of California are anticipated to be negatively impacted by warming temperatures, which will also cause shifts in seasonality of flow and a greater mismatch between timing of reservoir storage and water demand (Wang et al. 2018). Furthermore, studies suggest that warming temperatures will increase the risk of widespread, persistent droughts such as occurred in the 12th Century (Ault et al. 2016; Ault and St. George 2018), and thus, even more persistent perfect droughts should be anticipated in the future. Given the long-term record of natural hydrologic variability, along with current and projected changes in hydroclimate due to warming, perfect droughts such as 2012–2015 may become increasingly common, with the potential for even longer events to occur.

ACKNOWLEDGMENTS

Support for the research reported in this paper is from the California Department of Water Resources (Agreement number 4600011071). We thank numerous contributors of tree-ring data, and in particular, Dan Griffin for his updated blue oak chronologies, and Tony Caprio for assistance in updating his network of foxtail pine chronologies. We are grateful for the comments of Jeanine Jones on earlier drafts of this paper and for the helpful comments and suggestions from the associate editor and two anonymous reviewers. Support for the 20th Century Reanalysis Project dataset is provided by the U.S. Department of Energy, Office of Science Innovative and Novel Computational Impact on Theory and Experiment (DOE INCITE) Program, and Office of Biological and Environmental Research (BER), and by the National Oceanic and Atmospheric Administration Climate Program Office. We also acknowledge Dorian Burnette for his DIA analysis web tool (drought.memphis.edu) that was used for drought area assessment.

LITERATURE CITED

Abatzoglou, J.T., D.J. McEvoy, and K.T. Redmond. 2017. "The West Wide Drought Tracker: Drought Monitoring at Fine Spatial Scales." *Bulletin of the American Meteorological Society* 98: 1815–20.

Ault, T.R., J.S. Mankin, B.I. Cook, and J.E. Smerdon. 2016. "Relative Impacts of Mitigation, Temperature, and Precipitation on 21st-Century Megadrought Risk in the American Southwest." *Science Advances* 2: e1600873. https://doi.org/10.1126/sciadv.1600873.

Ault, T.R., and S. St. George. 2018. "Unraveling the Mysteries of Megadrought." *Physics Today* 71 (8): 44–50. https://doi.org/10.1063/PT.3.3997.

Barnston, A.G., and R.E. Livezey. 1987. "Classification, Seasonality and Persistence of Low-Frequency Atmospheric Circulation Patterns." *Monthly Weather Review* 115: 1083–126.

Belmecheri, S., F. Babst, E.R. Wahl, D.W. Stahle, and V. Trouet. 2016. "Millennium — Length Evaluation of Sierra Nevada Snowpack." *Nature Climate Change* 5: 748–52.

Biondi, F., C. Isaacs, M.K. Hughes, D.R. Cayan, and W.H. Berger. 2000. "The Near-1600 Dry/Wet Knock-Out: Linking Terrestrial and Nearshore Ecosystems." In *Proceedings of the 24th Annual Climate Diagnostics and Prediction Workshop*, edited by T. Barnston and E. O'Lenic, 76–79. Springfield, VA: National Technical Information Service, U.S. Department of Commerce.

Cleveland, W.S. 1979. "Robust Locally Weighted Regression and Smoothing Scatterplots." *Journal of the American Statistical Association* 74: 829–36.

Compo, G.P, J.S. Whitaker, P.D. Sardeshmukh, N. Matsui, R.J. Allan, X. Yin, B.E Gleason et al. 2011. "The Twentieth Century Reanalysis Project." *The Quarterly Journal of the Royal Meteorological Society* 137: 1–28. https://doi.org/10.1002/qj.776.

Cook, B.I., T.R. Ault, and J.E. Smerdon. 2015. "Unprecedented 21st Century Drought Risk in the American Southwest and Central Plains." *Science Advances* 1: e1400082. https://doi.org/10.1126/sciadv.1400082.

Cook, B.I., R. Seager, and J.E. Smerdon. 2014. "The Worst North American Drought Year of the Last Millennium: 1934." *Geophysical Research Letters* 41: 7298–305. https://doi.org/10.1002/2014GL061661.

Cook, E.R., D.M. Meko, and C.W. Stockton. 1997. "A New Assessment of Possible Solar and Lunar Forcing of the Bi-Decadal Drought Rhythm in the Western United States." *Journal of Climate* 10: 1343–56.

Cook, E.R., R. Seager, M.A. Cane, and D.W. Stahle. 2007. "North American Drought: Reconstructions, Causes and Consequences." *Earth Science Reviews* 81: 93–134.

Cook, E.R., R. Seager, R.R. Heim, R.S. Vose, C. Herweijer, and C. Woodhouse. 2010. "Megadroughts in North America: Placing IPCC Projections of Hydroclimatic Change in a Long-Term Paleoclimate Context." *Journal of Quaternary Science* 25: 48–61. https://doi.org/10.1002/jqs.1303.

Cook, E.R., C.A. Woodhouse, C.M. Eakin, D.M. Meko, and D.W. Stahle. 2004. "Long-Term Aridity Changes in the Western United States." *Science* 306: 1015–18.

Daly, C., M. Halbleib, J.I. Smith, W.P. Gibson, M.K. Doggett, G.H. Taylor, J. Curtis, and P.P. Pasteris. 2008. "Physiographically-Sensitive Mapping of Temperature and Precipitation across the Conterminous United States." *International Journal of Climatology* 28: 2031–64. https://doi.org/10.1002/joc.1688.

Dettinger, M.D., D.R. Cayan, H.F. Diaz, and D.M. Meko. 1998. "North-south Precipitation Patterns in Western North America on Interannual-to-Decadal Timescales." *Journal of Climate* 11: 3095–111.

Fritts, H.C., J. Guiot, and G.A. Gordon. 1990. "Verification." In *Methods of Dendrochronology: Applications in the Environmental Sciences*, edited by E.R. Cook, and L.A. Kairiukstis, 178–85. Dordrecht, The Netherlands: Kluwer Academic Publishers.

Gottlieb, R., and M. FitzSimmons. 1991. *Thirst for Growth: Water Agencies as Hidden Government in California*. Tucson, AZ: University of Arizona Press.

Griffin, D., and K.J. Anchukaitis. 2014. "How Unusual is the 2012–2014 California Drought?" *Geophysical Research Letters* 41 (24): 9017–23. https://doi.org/10.1002/2014GL062433.

Grinsted, A., J.C. Moore, and S. Jevrejeva. 2004. "Application of the Cross Wavelet Transform and Wavelet Coherence to Geophysical Time Series." *Nonlinear Processes in Geophysics* 11: 561–66.

Hurrell, J.W. 1995. "Decadal Trends in the North Atlantic Oscillation: Regional Temperatures and Precipitation." *Science* 269: 676–79. https://doi.org/10.1126/science.269.5224.676.

Kalnay, E., M. Kanamitsu, R. Kistler, W. Collins, D. Deaven, L. Gandin, M. Iredell et al. 1996. The NCEP/NCAR 40-Year Reanalysis Project. *Bulletin of the American Meteorological Society* 77: 437–70. https://www.esrl.noaa.gov/psd/.

Kipmueller, K.F., and M.W. Salzer. 2010. "Linear Trend and Climate Response of Five-Needle Pines in the Western United States Related to Treeline Proximity." *Canadian Journal of Forest Research* 40: 134–42. https://doi.org/10.1139/X09-187.

Lund, J., J. Medellin-Azuara, J. Durand, and K. Stone. 2018. "Lessons from California's 2012–2016 Drought." *Journal of Water Resources Planning and Management* 144: 2012–16. https://doi.org/10.1061/(ASCE)WR.1943-5452.0000984.

MacDonald, G.M., K.V. Krememetski, and H.G. Hidalgo. 2008. "Southern California and the Perfect Drought: Simultaneous Prolonged Drought in Southern California and the Sacramento and Colorado River Systems." *Quaternary International* 188: 11–23. https://doi.org/10.1016/j.quaint.2007.06.027.

Mann, M.E., Z. Zhang, M.K. Hughes, R.S. Bradley, S.K. Miller, S. Rutherford, and F. Ni. 2008. "Proxy-Based Reconstructions of Hemispheric and Global Surface Temperature Variations over the Past Two Millennia." *Proceedings of the National Academy of Sciences of the United States of America* 105: 13252–57. https://doi.org/10.1073/pnas.0805721105.

Margulis, S.A., G. Cortés, M. Girotto, L.S. Huning, D. Li, and M. Durand. 2016. "Characterizing the Extreme 2015 Snowpack Deficit in the Sierra Nevada (USA) and the Implications for Drought Recovery." *Geophysical Research Letters* 43: 6341–49. https://doi.org/10.1002/2016GL068520.

Martinez, W.L., and A.R. Martinez. 2002. *Computational Statistics Handbook with MATLAB*. New York: Chapman & Hall/CRC.

Meko, D. 1997. "Dendroclimatic Reconstruction with Time Varying Predictor Subsets of Tree Indices." *Journal of Climate* 10: 687–96.

Meko, D.M., D.W. Stahle, D. Griffin, and T.A. Knight. 2011. "Inferring Precipitation-Anomaly Gradients from Tree Rings." *Quaternary International* 235: 89–100.

Meko, D.M., M.D. Therrell, C.H. Baisan, and M.K. Hughes. 2001. "Sacramento River Flow Reconstructed to A.D. 869 from Tree Rings." *Journal of the American Water Resources Association* 37: 1029–40.

Meko, D.M., C.A. Woodhouse, C.H. Baisan, T. Knight, J.J. Lukas, M.K. Hughes, and M.W. Salzer. 2007. "Medieval Drought in the Upper Colorado River Basin." *Geophysical Research Letters* 34: L10705. https://doi.org/10.1029/2007GL029988.

Meko, D.M., C.A. Woodhouse, and E.R. Bigio. 2018. "Southern California Tree-Ring Study." Final Report to California Department of Water Resources, Agreement 4600011071. https://cwoodhouse.faculty.arizona.edu/content/california-department-water-resources-studies

Meko, D.M., C.A. Woodhouse, and R. Touchan. 2014. "Klamath/San Joaquin/Sacramento Hydroclimatic Reconstructions from Tree Rings." Final Report to California Department of Water Resources. Agreement 4600008850. https://cwoodhouse.faculty.arizona.edu/content/california-department-water-resources-studies

Michaelsen, J. 1987. "Cross-Validation in Statistical Climate Forecast Models." *Journal of Climate and Applied Meteorology* 26: 1589–600.

Mitchell, Jr., J.M., B. Dzerdzeevskii, H. Flohn, W.L. Hofmeyr, H.H. Lamb, K.N. Rao, and C.C. Walleen. 1966. "Climatic Change, Technical Note No. 79." Report of a Working Group of the Commission for Climatology No. 195 TP 100. Geneva, Switzerland: World Meteorological Organization.

Palmer, W.C.1965. "Meteorological Drought." U.S. Weather Bureau Research Paper 45, 58 pp.

Quadrelli, R., and J.M. Wallace. 2004. "A Simplified Linear Framework for Interpreting Patterns of Northern Hemisphere Wintertime Climate Variability." *Journal of Climate* 17: 3728–44.

Rayner, N.A., D.E. Parker, E.B. Horton, C.K. Folland, L.V. Alexander, D.P. Rowell, E.C. Kent, and A. Kaplan. 2003. "Global Analyses of Sea Surface Temperature, Sea Ice, and Night Marine Air Temperature since the Late Nineteenth Century." *Journal of Geophysical Research* 108 (D14): 4407. https://doi.org/10.1029/2002JD002670.

Routson, C.C., J.T. Overpeck, C.A. Woodhouse, and W.F. Kenney. 2016. "Three Millennia of Southwestern North American Dustiness and Future Implications." *PLoS ONE* 11 (2): e0149573. https://doi.org/10.1371/journal.pone.0149573.

Stahle, D.W., E.R. Cook, M.K. Cleaveland, M.D. Therrell, D.M. Meko, and H.D. Grissino-Mayer. 2000. "Tree-Ring Data Document 16th Century Megadrought over North America." *Eos, Transactions American Geophysical Union* 81: 121–25. https://doi.org/10.1029/00EO00076.

Stine, S. 1994. "Extreme and Persistent Drought in California and Patagonia during Medieval Time." *Nature* 369: 546–49.

Thompson, D.W.J., and J.M. Wallace. 1998. "The Arctic Oscillation Signature in the Wintertime Geopotential Height and Temperature Fields." *Geophysical Research Letters* 25: 1297–300.

Trouet, V., H.F. Diaz, E.R. Wahl, A.E. Viau, R. Graham, N. Graham, and E.R. Cook. 2013. "A 1500-Year Reconstruction of Annual Mean Temperature for Temperate North America on Decadal-to-Multidecadal Time Scales." *Environmental Research Letters* 8: 024008. https://doi.org/10.1088/1748-9326/8/2/024008.

Udall, B., and J.T. Overpeck. 2017. "The Twenty-First Century Colorado River Hot Drought and Implications for the Future." *Water Resources Research* 53: 2404–18. https://doi.org/10.1002/2016WR019638.

Visbeck, M.H., J.W. Hurrell, L. Polvani, and H.M. Cullen. 2001. "The North Atlantic Oscillation: Past, Present, and Future." *Proceedings of the National Academy of Sciences of the United States of America* 98 (23): 12876–77. https://doi.org/10.1073/pnas.231391598

Wang, J., H. Yin, E. Reyes, T. Smith, and F. Chung.2018. "Mean and Extreme Climate Change Impacts on the State Water Project." California's Fourth Climate Change Assessment. Publication Number: CCCA4-EXT-2018-004.

Weisberg, S. 1985. *Applied Linear Regression* (Second Edition). New York: John Wiley.

Williams, A.P., R. Seager, J.T. Abatzoglou, B.I. Cook, J.E. Smerdon, and E.R. Cook. 2015. "Contribution of Anthropogenic Warming to California Drought during 2012–2014: Global Warming and California Drought." *Geophysical Research Letters* 42: 6819–28. https://doi.org/10.1002/2015GL064924.

Wilson, R., K. Anchukaitis, K.R. Briffa, U. Büntgen, E. Cook, R. D'Arrigo, N. Davi et al. 2016. "Last Millennium Northern Hemisphere Summer Temperatures from Tree Rings: Part I: The Long Term Context." *Quaternary Science Reviews* 134: 1–18. https://doi.org/10.1016/j.quascirev.2015.12.005.

Wise, E.K. 2010. "Spatiotemporal Variability of the Precipitation Dipole Transition Zone in the Western United States." *Geophysical Research Letters* 37 (L07706). https://doi.org/10.1029/2009GL042193.

Wolter, K., and M.S. Timlin. 2011. "El Nino/Southern Oscillation Behavior since 1871 as Diagnosed in an Extended Multivariate ENSO Index (MEI.ext)." *International Journal of Climatology* 31: 1074–87. https://doi.org/10.1002/joc.2336.

Woodhouse, C.A., D.M. Meko, G.M. MacDonald, D.W. Stahle, and E.R. Cook. 2010. "A 1200-Year Perspective on the 21st Century Drought in Southwestern North America." *Proceedings of the National Academy of Sciences of the United States of America* 107: 21283–88.